

1 **TITLE:** *TcHRG* plays a central role in orchestrating heme uptake in *Trypanosoma cruzi*  
2 epimastigotes.

3

4 **RUNNING TITTLE:** The uptake of Hemoglobin-derived heme is mediated by *TcHRG* in  
5 *Trypanosoma cruzi* epimastigotes.

6

7

8

9 **AUTHORS:** Evelyn Tevere<sup>1</sup>, Cecilia Beatriz Di Capua<sup>1</sup>, Nathan Michael Chasen<sup>2</sup>, Ronald Drew  
10 Etheridge<sup>2</sup> and Julia Alejandra Cricco<sup>1,3\*</sup>.

11

12 **Affiliation:**

13 <sup>1</sup>Instituto de Biología Molecular y Celular de Rosario (IBR), Consejo Nacional de Investigaciones  
14 Científicas y Técnicas (CONICET)—Facultad de Ciencias Bioquímicas y Farmacéuticas,  
15 Universidad Nacional de Rosario (UNR), Rosario, Argentina

16 <sup>2</sup>Department of Cellular Biology, Center for Tropical and Emerging Global Diseases (CTEGD),  
17 University of Georgia, Athens, Georgia, USA

18 <sup>3</sup>Área Biofísica, Departamento de Química Biológica, Facultad de Ciencias Bioquímicas y  
19 Farmacéuticas, Universidad Nacional de Rosario (UNR), Rosario, Argentina

20 \* **CORRESPONDING AUTHOR:** Julia A. Cricco

21 **E-mail:** [cricco@ibr-conicet.gov.ar](mailto:cricco@ibr-conicet.gov.ar)

22

23

24

25 **KEYWORDS:** *Trypanosoma cruzi*, Chagas disease, heme, hemoglobin, heme transport, HRG

26

27

28

29

30

31 **ABSTRACT**

32 *Trypanosoma cruzi*, a heme auxotrophic parasite, can control intracellular heme content by  
33 modulating *TcHRG* expression when a free heme source is added to axenic culture. Herein, we  
34 explore the role of *TcHRG* protein in regulating the uptake of heme derived from hemoglobin  
35 in epimastigotes. It was found that the parasite's endogenous *TcHRG* (protein and mRNA)  
36 responds similarly to bound (hemoglobin) and free (hemin) heme. Additionally, the  
37 overexpression of *TcHRG* leads to an increase in intracellular heme content. The localization  
38 of *TcHRG* is also not affected in parasites supplemented with hemoglobin as the sole heme  
39 source. Endocytic null epimastigotes do not show a significant difference in growth profile,  
40 intracellular heme content and *TcHRG* protein accumulation compared to WT when feeding  
41 with hemoglobin or hemin as a source of heme. These results suggest that the uptake of  
42 hemoglobin-derived heme likely occurs through extracellular proteolysis of hemoglobin *via*  
43 the flagellar pocket, and this process is governed by *TcHRG*. In sum, *T. cruzi* epimastigotes  
44 controls heme homeostasis by modulating *TcHRG* expression independently of the source of  
45 available heme.

46

## 47 **INTRODUCTION**

48 *Trypanosoma cruzi* is the causative agent of Chagas disease, which is a widespread parasitic  
49 disease in the Americas [1]. This parasite undergoes a complex life cycle, which involves a  
50 mammalian host and a triatomine insect vector. *T. cruzi*, like other trypanosomatids that cause  
51 neglected diseases in humans such as *Trypanosoma brucei* and *Leishmania spp.*, are heme  
52 auxotrophic [2,3] and rely on obtaining this essential cofactor from their hosts or vectors. In  
53 the triatomine midgut, hemoglobin (Hb) derived from the bloodmeal is subjected to  
54 proteolysis, leading to the release of the heme moiety. Therefore, *T. cruzi* epimastigotes in  
55 their natural habitat encounter both Hb bound and free heme.

56 *In vitro* studies have shown that epimastigotes are able to incorporate both free and Hb  
57 derived heme to supply its metabolic requirements. Evidence suggests that, although  
58 internalized following different kinetics or pathways, both molecules are ultimately stored in  
59 reservosomes [4] which are lysosome-related organelles only present *T. cruzi* epimastigotes.  
60 It has been established that trans-membrane proteins belonging to the Heme Response Gene  
61 (HRG) family [5] are involved in the transport of heme from the environment in  
62 trypanosomatids. Several HRG family members have been described in trypanosomatids, for  
63 example LHR1 (*Leishmania Heme Response 1*) in *Leishmania amazonensis* [6–8], *TbHRG*

64 (*Trypanosoma brucei* Heme Responsive Gene) in *T. brucei* [9,10], and *TcHRG* (previously named  
65 *TcHTE*, *Trypanosoma cruzi* Heme Transport Enhancer) in *T. cruzi* [11,12]. Recently we reported  
66 a direct relationship between *TcHRG* and heme uptake based on the expression profile of the  
67 endogenous *TcHRG* gene and intracellular heme status. *TcHRG* (mRNA and protein) is mainly  
68 detected in the replicative life cycle stages of *T. cruzi* (epimastigote and amastigote), in which  
69 heme uptake is observed [11]. Also, *TcHRG* is highly expressed when epimastigotes are  
70 incubated with low or scarce levels of heme and becomes undetectable when intracellular  
71 heme reaches an optimal range. This suggests that epimastigotes can sense intracellular heme  
72 and modulate *TcHRG* expression to control free heme uptake [12].

73 On the other hand, Hb uptake *via* receptor-mediated endocytosis at the flagellar pocket (FP)  
74 was demonstrated in *T. brucei* [13] and *Leishmania spp.* [14,15], but these endocytic  
75 phenomenon through the FP have not been observed in *T. cruzi*. Moreover, it has not been  
76 found any specific cargo receptor in this parasite. Instead, *T. cruzi* has a specialized organelle  
77 called the cytotosome-cytopharynx complex (SPC) which is involved nutrient acquisition. The  
78 SPC is an invagination of the plasma membrane at the anterior end of the cell, which  
79 penetrates the cytoplasm towards the posterior end of the cell [16]. In the epimastigote stage,  
80 endocytosed proteins and lipids enters the cell through the cytotosome, are transported *via*  
81 endolysosomal vesicles through the cytopharynx and are finally stored in reservosomes at the  
82 posterior end of the cell [17]. The SPC and the reservosomes are absent in *T. brucei* and  
83 *Leishmania spp.*, constituting other relevant differences between them and *T. cruzi*.

84 In this report, we explored the utilization of Hb as a heme source in epimastigotes of *T. cruzi*  
85 and examined the role of *TcHRG* in Hb-derived heme homeostasis by analyzing endogenous  
86 *TcHRG* expression, the effect of the overexpression of *rTcHRG*, and the abolition of  
87 endocytosis when cultured in Hb-supplemented medium. We show that endogenous *TcHRG*  
88 responded similarly to Hb as it did to free heme (added as hemin) at both the mRNA and  
89 protein level. Also, the intracellular heme content was increased in parasites that overexpress  
90 recombinant *TcHRG* and was not affected in endocytic-null parasites when Hb was used as a  
91 heme source. Our results support an extended model for heme homeostasis in *T. cruzi*  
92 epimastigotes that includes both heme sources. We postulate that “free heme” obtained after  
93 extracellular Hb degradation is the main pathway for Hb-derived heme uptake in  
94 epimastigotes and it is enhanced and controlled by the heme transporter *TcHRG*.

95

## 96 RESULTS

### 97 *TcHRG* responds to hemoglobin

98 To study the effect of Hb as heme source, we followed the growth profile of WT epimastigotes  
99 comparing both free heme (added as hemin) and Hb-derived heme. Briefly, parasites cultured  
100 in LIT-10% FBS + 5  $\mu$ M hemin [12] were challenged to heme starvation for 48 h and then  
101 transferred to media supplemented with 5, 20, and 50  $\mu$ M hemin, with 1.25, 5, and 12.5  $\mu$ M  
102 Hb (equivalent to 5, 20, and 50  $\mu$ M heme as Hb) and without any source of heme added (0  
103  $\mu$ M). The number of parasites per ml was measured every day for 14 days, performing a  
104 dilution in fresh media on the seventh day. Along the 14 days, the growth of Hb-supplemented  
105 epimastigotes was slightly inferior compared to the standard condition (LIT-10% FBS + 5  $\mu$ M  
106 hemin). During the second week, Hb-supplemented epimastigotes displayed similar growth  
107 profiles among each other, in stark contrast with the negative effect observed on  
108 epimastigotes' growth at higher hemin concentrations, 20 and 50  $\mu$ M. (Fig. 1A and [12]). We  
109 did not detect any alteration in parasite morphology when the Hb-supplemented  
110 epimastigotes were observed under an optical microscope, contrary to the alterations caused  
111 by equivalent free heme concentrations added as hemin [12].

112 We then evaluated *TcHRG* protein accumulation by Western blotting on samples taken after  
113 one-, three-, seven-, and fourteen-days post addition of a heme source. To recognize the  
114 endogenous protein, anti-*TcHRG* polyclonal antibodies were used (named anti-*TcHTE* in [12]).  
115 Fig. 1B shows that *TcHRG* corresponding signal was detected as an intense band in parasites  
116 incubated without heme throughout the assay. Also, a weak signal was observed in parasites  
117 incubated with 1.25  $\mu$ M Hb on day 1. *TcHRG* was almost undetectable since day 1 in the  
118 remaining conditions.

119 In addition, *TcHRG* expression was also examined through qRT-PCR analysis 24 h upon  
120 treatment with 5  $\mu$ M hemin or 1.25  $\mu$ M Hb (Fig. 1C). Consistently, *TcHRG* mRNA amounts  
121 remained constant in heme-starved epimastigotes. Likewise, significant reductions of  
122 approximately 50% and 25% in mRNA levels were observed 24 h after treatment with 5  $\mu$ M  
123 heme as hemin and Hb, respectively.

124 On the other hand, the intracellular heme content (IHC) of parasites supplemented with 5  $\mu$ M  
125 hemin or 1.25  $\mu$ M Hb for 48 and 96 h was analyzed. Fig. 1D shows that, after 48 h of treatment,  
126 parasites incubated with hemin reached  $2.6 \pm 0.1$  nmol heme/ $10^9$  parasites, meanwhile  
127 parasites incubated with Hb showed a significant lower amount of IHC, about  $1.2 \pm 0.1$  nmol

128 heme/ $10^9$  parasites, approximately 50%. After 96 h, parasites incubated with hemin  
129 maintained IHC and those incubated with Hb increased their IHC to  $2.1 \pm < 0.1$  nmol heme/ $10^9$   
130 parasites, similar to hemin treated ones.

131 In summary, epimastigotes tolerated higher heme concentrations when Hb was the source.  
132 They reached similar IHC when incubated with equivalent concentrations of heme using both  
133 sources, presumably the optimal intracellular heme content under these experimental  
134 conditions. However, epimastigotes incubated with Hb required more time to reach IHC than  
135 those incubated with hemin. Additionally, endogenous *TcHRG* (protein and mRNA)  
136 accumulation generated by heme starvation underwent a significant decrease in response to  
137 the addition of Hb.

### 138 **Endocytic null parasites maintain heme homeostasis**

139 To gain insight in the uptake of Hb-derived heme, we evaluated what happened in  
140 epimastigotes unable to perform endocytosis when incubated with Hb as a heme source. We  
141 used  $\Delta TcAct2$  epimastigotes from Y strain, in which the gene for the actin isoform 2, which is  
142 necessary for SPC-mediated endocytosis, was deleted (manuscript in preparation). The WT  
143 line and a line in which the *TcAct2* gene was added back (complemented) with a Ty tag  
144 (*TcAct2.Ty*) were used as controls.

145 First, to evaluate the behavior of the endocytic null parasites, we registered the growth  
146 performance of the three cell lines (after 48 h of heme starvation treatment) in a medium  
147 supplemented with 5  $\mu$ M hemin, 1.25  $\mu$ M Hb, or without the addition of any source of heme  
148 (0  $\mu$ M) for seven days. As shown in Figure 2A, the growth of the  $\Delta TcAct2$  was comparable in  
149 both heme sources, although the maximal parasite/ml number was slightly less when  
150 compared to the WT and *TcAct2.Ty* lines in same conditions. Additionally, the growth of the  
151 three lines was severely impaired when no heme source was added. Endogenous *TcHRG*  
152 expression was also evaluated by Western blotting after 48 h of incubation in the conditions  
153 mentioned above. As shown in Figure 2B, *TcHRG* signal in WT,  $\Delta TcAct2$ , and *TcAct2.Ty* was  
154 clearly detected in samples incubated without the addition of heme and in Hb-supplemented  
155 ones. Also, a very weak signal was observed in WT,  $\Delta TcAct2$ , and *TcAct2.Ty* parasites  
156 supplemented with hemin.

157 Additionally, we analyzed the IHC of these parasites after 48 h of incubation with both heme  
158 sources and without heme. Figure 2C shows that IHC profiles were similar in the three lines.  
159 All of them reached an IHC of about 2.3-2.6 nmol heme/ $10^9$  parasites in hemin-supplemented

160 media, while when they were incubated with Hb the IHC was significantly lower, about 1.3-  
161 1.8 nmol heme/10<sup>9</sup> parasites. Also, when no heme source was added (0 μM), the three  
162 variants presented IHC that were significantly lower as compared to parasites treated with  
163 hemin, about of 0.9 nmol heme/10<sup>9</sup> parasites.

164 In summary, endocytic null parasites presented a minimal growth defect with both heme  
165 source (hemin or Hb) compared to control lines. These parasites presented a protein  
166 expression pattern of *TcHRG* comparable to Dm28c WT epimastigotes under similar  
167 treatments. Additionally, IHC of endocytic null parasites was comparable to the WT and  
168 complemented line in all conditions evaluated here.

169

### 170 **Overexpression of *TcHRG* contributes to heme transport in Hb-supplemented parasites**

171 To confirm the role of *TcHRG* in the uptake of heme derived from Hb, we analyzed the IHC of  
172 epimastigotes overexpressing *rTcHRG.His-GFP* (*rTcHRG*) when supplemented with Hb as a  
173 heme source. Epimastigotes transfected with *pTcIndexGW.TcHRG.His-GFP* or *pTcIndex* (as a  
174 control) were cultured for 48 h in media supplemented with 5 μM heme as hemin or as Hb.  
175 Figure 3A shows that epimastigotes expressing *rTcHRG* incubated with Hb presented an IHC  
176 significantly higher compared to control parasites,  $2.2 \pm 0.1$  vs.  $1.2 \pm 0.1$  nmol heme/10<sup>9</sup>  
177 parasites, respectively. Also, the presence of *rTcHRG* was verified by Western blotting using  
178 polyclonal anti-GFP antibodies, as shown in Fig. 3B. Epimastigotes overexpressing *rTcHRG*  
179 incubated with Hb exhibited an incremental increase in IHC analogous to what was reported  
180 using hemin as heme source (see Fig. 3A here and [11]).

181

### 182 **Endogenous *TcHRG* has a dual localization**

183 *rTcHRG.His-GFP* was localized in the FP region of recombinant epimastigotes [11], but the  
184 localization of endogenous *TcHRG* remained elusive. To address the later, first we performed  
185 immunofluorescence assays to detect *rTcHRG* in *rTcHRG.His-GFP* overexpressing parasites by  
186 super-resolution light microscopy using polyclonal anti-*TcHRG* antibodies as primary antibodies.  
187 Figure 4A shows that the signal corresponding to anti-*TcHRG* antibodies (red) overlapped with  
188 the green signal of *rTcHRG.His-GFP*, confirming that these antibodies specifically label *TcHRG*.  
189 Then, we used the same strategy to analyze the localization of endogenous *TcHRG* in WT  
190 parasites incubated with 5 μM hemin or 1.25 μM Hb for 48 h. Additionally, we took advantage

191 of concanavalin A to stain the parasite surface and the cytostome entrance[18]. As shown in  
192 Figure 4B, a principal band-shaped signal was observed near the kinetoplast, consistent with  
193 a localization in FP region. Additionally, punctual signals were found throughout the  
194 cytoplasm, the pattern of these signals suggested that endogenous protein could be localized  
195 (at least partially) to the mitochondrion. To corroborate this, we used MitoTracker to stain the  
196 parasite mitochondrion as shown in Fig 4C. The green signal of *TcHRG* partially overlapped  
197 with the red signal of MitoTracker, suggesting that endogenous *TcHRG* could be localized also  
198 to the mitochondrial membrane or close to it. On the other hand, we did not observe any  
199 difference in the signal patterns of endogenous *TcHRG* between Y and Dm28c strains nor the  
200 incubation conditions (Dm28c not shown) (Fig 4B). In summary, as schematized in Figure 4D,  
201 endogenous *TcHRG* was found in the proximity of the kinetoplast, which is compatible with  
202 the position of FP, and partially overlapping with the mitochondrion, while *rTcHRG*.His-GFP  
203 was observed mainly in the FP region.

204

## 205 **DISCUSSION**

206 It was proposed that Hb is the main source of heme *in vivo* for epimastigotes given that it can  
207 be obtained from erythrocyte lysis after a bloodmeal in the midgut of the triatomine vector.  
208 Then, to obtain heme from Hb, epimastigotes were thought to internalize protein bound heme  
209 *via* SPC, degrade it, and then utilize free-heme and peptides. However, conversely to *T. brucei*  
210 and *Leishmania spp.*, no specific receptor that mediates Hb endocytosis or putative ORF that  
211 may fulfill this function has been described or found in *T. cruzi* genome and very little is known  
212 about the endocytic process through the SPC. On the other hand, Hb can be degraded via  
213 external peptidases to release free heme and peptides, although triatomines present  
214 mechanisms to rapidly get rid of free heme to avoid oxidative damage [19]. In this work, we  
215 present a model for Hb-derived heme uptake, explaining the role of *TcHRG* in this process.  
216 The growth performance of epimastigotes was not affected when Hb was used as heme  
217 source in axenic culture, moreover, higher concentrations of Hb did not cause the same  
218 negative effect on growth as is observed when equivalent concentration of hemin was added  
219 [12]. This phenomenon may be explained because both sources are incorporated via different  
220 pathways or kinetics allowing the parasite to distribute and correctly store the cofactor,  
221 and/or because heme embedded within Hb produces less oxidative damage to the lipids and  
222 proteins of the plasma membrane as compared to free heme[20]. Additionally, the

223 concentration of intracellular heme differed between both heme sources during the first 48 h  
224 after they were added to the medium, but reached similar values at 96 h, supporting the idea  
225 that time is needed to degrade extracellular hemoglobin and thus release Hb-derived heme  
226 for uptake and intracellular utilization by epimastigotes.

227 *TcHRG* (formerly *TcHTE*) is an essential player in the control and regulation of free heme  
228 uptake, as its amount (both mRNA and protein) are adjusted according to the intracellular  
229 heme status[12]. Our results have shown that the *TcHRG* protein signal decreases when both  
230 heme sources are used; however, it is still detected 24 h – 48 h post Hb addition. Furthermore,  
231 mRNA levels dropped about 25 % with Hb whereas about 50 % with hemin, in both cases when  
232 the heme source was added after heme starvation. This behavior agrees with the observed  
233 intracellular heme levels and strongly suggest that, despite that how Hb-derived heme enters  
234 the cell, *TcHRG* plays a crucial role sensing intracellular heme and responding to it.

235 As mentioned before, Hb might be internalized via SPC however, the growth performance of  
236 endocytic null epimastigotes ( $\Delta TcAct2$ ) was similar in the presence of both heme sources,  
237 although the final parasite number was slightly lower as compared to WT and complemented  
238 (*TcAct2.Ty*) lines in the same conditions. This minor phenomenon is possibly due to the  
239 inability to obtain some additional minor nutrients by endocytosis. Regardless, when the  
240 intracellular heme concentration was measured in WT,  $\Delta TcAct2$  and *TcAct2.Ty* they all  
241 demonstrated a similar profile. Heme starvation caused a drop in the intracellular levels, and,  
242 although IHC was lower when Hb was used as heme source compared to hemin, the same  
243 behavior is observed in Dm28c epimastigotes. Independently of the heme source  
244 supplemented, endocytic null parasites exhibit similar growth with both and can reach WT  
245 intracellular heme levels, indicating that epimastigotes rely on mechanisms independent of  
246 endocytosis to take up heme from the environment. Importantly, the *TcHRG* protein is present  
247 at the same level in all three lines, being almost undetectable when hemin was used and still  
248 detected 48 h after the addition of Hb, confirming the role of this protein in control of heme  
249 homeostasis independently of the heme source. Additionally, the overexpression of *rTcHRG*  
250 led to an increase in the intracellular heme content in parasites supplemented with Hb  
251 comparable to the effect observed when hemin is used as free heme source [11]. These data  
252 suggest that the incorporation of free heme and heme derived from Hb could proceed by same  
253 mechanism but with different timing. One possible explanation for this phenomenon is that  
254 the parasite may contribute (at least partially) to extracellular Hb breakdown *via* secreted [21]

255 or surface proteases [22], then “free” heme derived from Hb degradation required extra time  
256 to be incorporated compared to the addition of hemin to the medium. The hypothesis that  
257 parasite proteases might contribute to protein digestion in the lumen of the triatomine midgut  
258 was suggested by García and colleagues, although the details of this process remain poorly  
259 understood [23].

260 Taking advantage of super-resolution microscopy, it was possible to observe recombinant as  
261 well as endogenous *TcHRG* using anti-*TcHRG* antibodies. *rTcHRG* was detected in the proximity  
262 of the FP as previously reported [11], meanwhile the endogenous protein signal was visualized  
263 for the first time, and it was localized next to the FP (close to the kinetoplast) and as multiple  
264 puncta in the cytoplasm. The localization of *rTcHRG* signal only in FP region could be a  
265 consequence of the structure of the fusion protein where, probably, the presence of the GFP  
266 moiety would prevent the migration of the protein to other cellular regions. Interestingly, the  
267 intracellular signal of *TcHRG* did not change according to the heme source. Its localization in  
268 the FP region supports that *TcHRG* plays a role in both heme uptake and homeostasis control,  
269 in agreement with the hypothesis that permeases and transporters in trypanosomatids also  
270 play roles in sensing [24]. The intracellular signals of *TcHRG* exhibited partial superposition  
271 with mitochondrial signal, suggesting a more complex role for this protein; probably involved  
272 in intracellular heme trafficking or sensing. This localization differs from the observed in other  
273 trypanosomatids where HRGs were observed in intracellular vesicles [6,9], but in all cases it  
274 was suggested a role in heme trafficking. One possible role of mitochondrial *TcHRG* could be  
275 the sensing of intracellular heme status and/or intracellular heme trafficking in this organelle.  
276 Results presented in this work indicate that the main heme entrance pathway in *T. cruzi*  
277 epimastigotes is the same for both heme sources (hemin and Hb) and it is mediated by *TcHRG*.  
278 We explain how epimastigotes control heme homeostasis regulated by *TcHRG* when Hb is  
279 available as a heme source, as summarized in Figure 5. Hb can be externally degraded by  
280 surface or secreted proteases produced by either the parasite or the insect vector [23], and  
281 free heme uptake is enhanced by *TcHRG* at the FP region. Although not examined in this study,  
282 Hb might be endocytosed *via* SPC. More importantly, independent of the heme source,  
283 epimastigotes sense intracellular heme status presumably *via* intracellular *TcHRG*. Once the  
284 optimal concentration range is reached, a still unknown signal may trigger *TcHRG* to turn off  
285 to avoid further heme uptake which is likely toxic, as was previously reported [12].

286 In summary, we present here an extended model to explain Hb-derived heme uptake in  
287 epimastigotes of *T. cruzi*. Our results reinforce the relevance of TcHRG in the crucial process  
288 of heme transport and homeostasis independently of the source, constituting a key player in  
289 *Trypanosoma cruzi*. For these reasons, elucidation of the complete heme uptake pathways  
290 will contribute to the identification of other novel essential proteins and generate new  
291 strategies for Chagas' disease treatment.

292

### 293 **Experimental procedures**

294 **Reagents:** Fetal Bovine Serum (FBS) (Internegocios SA) was heat-inactivated at 56°C for an  
295 hour prior to use. Hemin (Frontier Scientific) solution stock was prepared as previously  
296 described (Merli 2016). Heme concentration in hemin stock solution was confirmed by  
297 spectroscopic measurements at 385 nm,  $\epsilon^{385} = 58400 \text{ M}^{-1}\text{cm}^{-1}$  [25]. Lyophilized bovine Hb  
298 (Sigma) stock solution was prepared in PBS to a final concentration of 0.1 mM, sterilized by  
299 filtration using a 0.22  $\mu\text{m}$  syringe disposable filter and stored at -80°C. Concentration in Hb  
300 stock was confirmed by indirectly measuring heme by basic piridine method described below,  
301 considering that one Hb molecule contains four heme molecules. Integrity of Hb secondary  
302 structure was verified by circular dichroism spectroscopy and SDS-PAGE.

303 **Parasites:** *T. cruzi* Dm28c strain was used to analyze parasite growth, expression of  
304 endogenous TcHRG (WT) and to study the effect of rTcHRG overexpression and localization in  
305 medium supplemented with Hb (pLEW13 pTcIndex and pLEW13 pTcIndex.GW.TcHRG.6His-  
306 GFP lines). Analysis of endocytosis suppression was performed using *T. cruzi* Y strain (WT,  
307  $\Delta\text{TcAct2}$ , and *TcAct2.Ty* lines).

308 Epimastigotes were routinely maintained in mid-log phase by periodic dilutions in Liver  
309 Infusion Tryptose (LIT) medium supplemented with 10% heat inactivated FBS (LIT-10% FBS)  
310 and 5  $\mu\text{M}$  hemin (Pagura 2020), at 28 °C. Prior to each experiment described in this work,  
311 epimastigotes were collected, washed with PBS and transferred to LIT-10% FBS without heme  
312 source added for 48 h ("heme starvation").

313 **Growth curves:** Dm28c WT epimastigotes routinely maintained LIT-10% FBS + 5  $\mu\text{M}$  hemin  
314 were challenged to heme starvation for 48 h. Then, parasites were collected by centrifugation  
315 at 3500 g for 5', washed with PBS and transferred to LIT-10% FBS without heme (0  $\mu\text{M}$ ) or  
316 supplemented with 5, 20, or 50  $\mu\text{M}$  hemin or 1.25, 5, and 12.5  $\mu\text{M}$  Hb (equivalent to 5, 20, or  
317 50  $\mu\text{M}$  heme as Hb). The number of cells was monitored daily for 14 days. On day 7, cultures

318 were diluted to the parasite concentration measured on day 1 and the growth curve was  
319 followed for another week. On the first-, third-, seventh-, and fourteenth-days parasites  
320 samples were collected and prepared for Western Blot analysis as described below and the  
321 morphology was verified by optical microscopy. Similarly, Y epimastigotes (WT,  $\Delta TcAct2$ , and  
322  $TcAct2.Ty$  lines) were heme starved for 48 h and transferred to LIT-10% FBS without (0  $\mu M$ ) or  
323 supplemented with 5  $\mu M$  hemin or 1.25  $\mu M$  Hb. The growth curve was followed for one week.  
324 The results are expressed as mean  $\pm$  SD of three independent experiments. Cell growth was  
325 monitored by cell counting using Wiener lab. Counter 19 Auto Hematology Analyzer (Wiener  
326 Laboratorios SAIC, Rosario, Argentina) configured for parasite number measurements and  
327 Neubauer chamber.

328 **Western blot:** Total protein from cell-free extracts were obtained and processed as described  
329 previously [12] with minor modifications.  $5 \times 10^6$  cells/well were resolved by electrophoresis  
330 on a 12% SDS-polyacrylamide gel.  $TcHRG$  detection was performed with rabbit polyclonal anti-  
331  $TcHRG$  antibodies (1:10000).  $rTcHRG.6His-GFP$  expression was corroborated using anti-GFP  
332 antibodies (1:1000) (Santa Cruz Biotechnology, Inc.). In both cases, peroxidase-labeled anti-  
333 rabbit IgG (1:30000) (Calbiochem) were used as secondary antibodies. Loading control was  
334 performed with anti- $\alpha$ -tubulin clone TAT-1 antibodies (a gift from K. Gull, University of Oxford,  
335 U.K.), using peroxidase-labeled anti-mouse IgG antibodies (1:5000) (GE Healthcare) as  
336 secondary antibodies. Bound antibodies were detected with ECL Prime Western Blotting  
337 Detection kit (GE Healthcare). Anti- $TcHRG$  antibodies were generated as described previously  
338 [12].

339 **RNA isolation, reverse transcription PCR (RT-PCR) and quantitative real-time PCR (qRT-PCR).**  
340 After heme starvation, Dm28c WT epimastigotes were collected, washed with PBS and  
341 challenged to grow in LIT-10% FBS without (0  $\mu M$ ) or supplemented with 5  $\mu M$  hemin or 1.25  
342  $\mu M$  Hb. Samples in triplicates were collected for RNA isolation prior transferring parasites to  
343 the different conditions ( $t_0$ ) and after 24 hours of incubation ( $t_{24}$ ). Total mRNA isolation,  
344 treatment and quantification was carried out as described previously (Pagura 2020). cDNAs  
345 were synthesized through a RT reaction (M-MuLV, Thermo-Scientific) using 0.5  $\mu g$  of total  
346 RNA. cDNA samples were used as template for Quantitative Real-time PCR performed in an  
347 Applied Biosystems StepOne™ Real-Time PCR System Thermal Cycling Block using the  
348 EvaGreen fluorescence quantification system (Solis BioDyne). qRT-PCR reaction was  
349 conducted as previously described (Pagura 2020). The results are expressed as mean  $\pm$  SD of

350 three technical replica from one representative of two independent experiments (biological  
351 replica).

352 **Immunofluorescence assays:** Epimastigotes (Y and Dm28c strains) are routinely grown in LIT-  
353 10% FBS + 5  $\mu$ M hemin were subjected to heme starvation for 48 h. Then, parasites were  
354 harvested, washed with PBS and transferred to LIT-10% FBS without (0  $\mu$ M) or supplemented  
355 with 5  $\mu$ M hemin or 1.25  $\mu$ M Hb for 48 h.

356 Mounted samples of epimastigotes for fluorescence imaging were prepared and labeled with  
357 10  $\mu$ g/ml rhodamine-conjugated concanavalin A (Vector Laboratories) as described previously  
358 (Chasen 2019). Polyclonal anti-*Tc*HRG antibodies were used as primary antibodies in WT and  
359 r*Tc*HRG.His-GFP overexpressing parasites. As secondary antibodies, goat anti-rabbit IgG Alexa  
360 Fluor 488 (Thermo Fisher) were used in WT epimastigotes, while goat anti-rabbit IgG Alexa  
361 Fluor 568 (Thermo Fisher) were used in r*Tc*HRG.His-GFP overexpressing parasites.  
362 MitoTracker<sup>TM</sup> Red CMXRos (Thermo Fisher) was used to dye epimastigotes mitochondria.

363 All the images were acquired with Zeiss Elyra S1 structured illumination microscope (Center  
364 for Tropical and Emerging Diseases Biomedical Microscopy Core, Athens, GA) and were  
365 processed using the ImageJ software.

366 **Heme content analysis:** After heme starvation, parasites were harvested, washed twice with  
367 PBS and transferred to the corresponding medium (supplemented with 5  $\mu$ M hemin, 1.25  $\mu$ M  
368 Hb, or without heme) for 48 h or 96 h. Epimastigotes were harvested and washed three times  
369 with PBS. Each determination required  $150 \times 10^6$  epimastigotes. Intracellular heme content of  
370 epimastigotes was determined by basic pyridine method described in Berry *et al.* [26],  
371 adapted in our laboratory to perform measurements in epimastigotes samples, as we  
372 described previously [27]. The results are expressed as mean  $\pm$  SD of three independent  
373 experiments (biological replicates), each containing two technical replicates.

374 **Statistical analysis:** All the assays were independently reproduced at least 2–3 times.  
375 Statistically significant differences between groups were analyzed using GRAPHPAD PRISM  
376 version 6.00 for Windows (GraphPad Software, San Diego, CA), as described in each  
377 experiment.

378

## 379 REFERENCES

380 1 Rassi, A. and Marcondes de Rezende, J. (2012) American trypanosomiasis (Chagas disease).  
381 Infect Dis Clin North Am **26**, 275–91.

- 382 2 Kořený, L., Lukeš, J. and Oborník, M. (2010) Evolution of the haem synthetic pathway in  
383 kinetoplastid flagellates: An essential pathway that is not essential after all? *Int J Parasitol* **40**,  
384 149–156.
- 385 3 Tripodi, K. E. J. J., Menendez Bravo, S. M. and Cricco, J. A. (2011) Role of heme and heme-  
386 proteins in trypanosomatid essential metabolic pathways. *Enzyme Res* **2011**, 873230.
- 387 4 Lara, F. A., Sant’Anna, C., Lemos, D., Laranja, G. A. T., Coelho, M. G. P., Reis Salles, I., Michel,  
388 A., Oliveira, P. L., Cunha-e-Silva, N., Salmon, D., et al. (2007) Heme requirement and  
389 intracellular trafficking in *Trypanosoma cruzi* epimastigotes. *Biochem Biophys Res Commun*  
390 **355**, 16–22.
- 391 5 Rajagopal, A., Rao, A. U., Amigo, J., Tian, M., Upadhyay, S. K., Hall, C., Uhm, S., Mathew, M. K.,  
392 Fleming, M. D., Paw, B. H., et al. (2008) Haem homeostasis is regulated by the conserved and  
393 concerted functions of HRG-1 proteins. *Nature* **453**, 1127–1131.
- 394 6 Huynh, C., Yuan, X., Miguel, D. C., Renberg, R. L., Protchenko, O., Philpott, C. C., Hamza, I. and  
395 Andrews, N. W. (2012) Heme uptake by *Leishmania amazonensis* is mediated by the  
396 transmembrane protein LHR1. *PLoS Pathog* **8**, 36.
- 397 7 Miguel, D. C., Flannery, A. R., Mitra, B. and Andrews, N. W. (2013) Heme uptake mediated by  
398 *lhr1* is essential for *leishmania amazonensis* virulence. *Infect Immun* **81**, 3620–3626.
- 399 8 Renberg, R. L., Yuan, X., Samuel, T. K., Miguel, D. C., Hamza, I., Andrews, N. W. and Flannery,  
400 A. R. (2015) The Heme Transport Capacity of LHR1 Determines the Extent of Virulence in  
401 *Leishmania amazonensis*. *PLoS Negl Trop Dis* **9**, e0003804.
- 402 9 Cabello-Donayre, M., Malagarie-Cazenave, S., Campos-Salinas, J., Gálvez, F. J., Rodríguez-  
403 Martínez, A., Pineda-Molina, E., Orrego, L. M., Martínez-García, M., Sánchez-Cañete, M. P.,  
404 Estévez, A. M., et al. (2016) Trypanosomatid parasites rescue heme from endocytosed  
405 hemoglobin through lysosomal HRG transporters. *Mol Microbiol* **101**, 895–908.
- 406 10 Horáková, E., Changmai, P., Vancová, M., Sobotka, R., Abbeele, J. Van Den, Vanhollebeke, B.  
407 and Lukeš, J. (2017) The *Trypanosoma brucei* Tb Hrg protein is a heme transporter involved in  
408 the regulation of stage-specific morphological. *J. Biol. Chem.* **292**, 6998–7010.
- 409 11 Merli, M. L., Pagura, L., Hernández, J., Barisón, M. J., Pral, M. F., Silber, A. M. and Cricco, J. A.  
410 (2016) The *Trypanosoma cruzi* Protein TcHTE Is Critical for Heme Uptake. *PLoS Negl Trop Dis*  
411 1–18.
- 412 12 Pagura, L., Tevere, E., Merli, M. L. and Cricco, J. A. (2020) A new model for *Trypanosoma cruzi*  
413 heme homeostasis depends on modulation of TcHTE protein expression. *Journal of Biological*  
414 *Chemistry, American Society for Biochemistry and Molecular Biology* **295**, 13202–13212.
- 415 13 Vanhollebeke, B., De Muylder, G., Nielsen, M. J., Pays, A., Tebabi, P., Dieu, M., Raes, M.,  
416 Moestrup, S. K. and Pays, E. (2008) A haptoglobin-hemoglobin receptor conveys innate  
417 immunity to *Trypanosoma brucei* in humans. *Science, United States* **320**, 677–681.
- 418 14 Sengupta, S., Tripathi, J., Tandon, R., Raje, M., Roy, R. P., Basu, S. K. and Mukhopadhyay, A.  
419 (1999) Hemoglobin endocytosis in *Leishmania* is mediated through a 46-kDa protein located  
420 in the flagellar pocket. *J Biol Chem, United States* **274**, 2758–2765.

- 421 15 Krishnamurthy, G., Vikram, R., Singh, S. B., Patel, N., Agarwal, S., Mukhopadhyay, G., Basu, S.  
422 K. and Mukhopadhyay, A. (2005) Hemoglobin receptor in Leishmania is a hexokinase located  
423 in the flagellar pocket. *Journal of Biological Chemistry* **280**, 5884–5891.
- 424 16 Milder, R. and Deane, M. P. (1969) The cytostome of *Trypanosoma cruzi* and *T. conorhini*. *J*  
425 *Protozool, United States* **16**, 730–737.
- 426 17 Porto-Carreiro, I., Attias, M., Miranda, K., De Souza, W. and Cunha-E-Silva, N. (2000)  
427 *Trypanosoma cruzi* epimastigote endocytic pathway: Cargo enters the cytostome and passes  
428 through an early endosomal network before storage in reservosomes. *Eur J Cell Biol* **79**, 858–  
429 869.
- 430 18 Chasen, N. M., Coppens, I. and Etheridge, R. D. (2020) Identification and Localization of the  
431 First Known Proteins of the *Trypanosoma cruzi* Cytostome Cytopharynx Endocytic Complex.  
432 *Front Cell Infect Microbiol* **9**, 1–15.
- 433 19 Graça-Souza, A. V., Maya-Monteiro, C., Paiva-Silva, G. O., Braz, G. R. C., Paes, M. C., Sorgine, M.  
434 H. F., Oliveira, M. F. and Oliveira, P. L. (2006) Adaptations against heme toxicity in blood-  
435 feeding arthropods. *Insect Biochem Mol Biol* **36**, 322–335.
- 436 20 Kumar, S. and Bandyopadhyay, U. (2005) Free heme toxicity and its detoxification systems in  
437 human. *Toxicol Lett* **157**, 175–188.
- 438 21 Bayer-Santos, E., Aguilar-Bonavides, C., Rodrigues, S. P., Cordero, E. M., Marques, A. F., Varela-  
439 Ramirez, A., Choi, H., Yoshida, N., Da Silveira, J. F. and Almeida, I. C. (2013) Proteomic analysis  
440 of *trypanosoma cruzi* secretome: Characterization of two populations of extracellular vesicles  
441 and soluble proteins. *J Proteome Res* **12**, 883–897.
- 442 22 Queiroz, R. M. L., Charneau, S., Motta, F. N., Santana, J. M., Roepstorff, P. and Ricart, C. A. O.  
443 (2013) Comprehensive proteomic analysis of *Trypanosoma cruzi* epimastigote cell  
444 surface proteins by two complementary methods. *J Proteome Res, United States* **12**, 3255–  
445 3263.
- 446 23 Garcia, E. S., Genta, F. A., De Azambuja, P. and Schaub, G. A. (2010) Interactions between  
447 intestinal compounds of triatomines and *Trypanosoma cruzi*. *Trends Parasitol* **26**, 499–505.
- 448 24 Landfear, S. M. and Zilberstein, D. (2019) Sensing What’s Out There – Kinetoplastid Parasites.  
449 *Trends Parasitol, Elsevier Ltd* **35**, 274–277.
- 450 25 Yuan, X., Rietzschel, N., Kwon, H., Walter Nuno, A. B., Hanna, D. A., Phillips, J. D., Raven, E. L.,  
451 Reddi, A. R. and Hamza, I. (2016) Regulation of intracellular heme trafficking revealed by  
452 subcellular reporters. *Proc Natl Acad Sci U S A* **113**, E5144-52.
- 453 26 Berry, E. a and Trumpower, B. L. (1987) Simultaneous determination of hemes a, b, and c from  
454 pyridine hemochrome spectra. *Anal Biochem* **161**, 1–15.
- 455 27 Merli, M. L., Cirulli, B. A., Menendez-Bravo, S. M. and Cricco, J. A. (2017) Heme A synthesis and  
456 CcO activity are essential for *Trypanosoma cruzi* infectivity and replication. *Biochem J, England*  
457 **474**, 2315–2332.
- 458

459 **Acknowledgments:** We are grateful to the government of the province of Santa Fe for  
460 awarding ET the "Mobility Scholarship with a Gender Perspective" (2022).

461

462 **Funding information:** The research leading to these results has, in part, received funding from  
463 UK Research and Innovation via the Global Challenges Research Fund under grant agreement  
464 'A Global Network for Neglected Tropical Diseases' grant number MR/P027989/1 to J.A.C.  
465 (2018-2022), and AGENCIA I+D+i (National Agency of Scientific Investigation, Technological  
466 Development Promotion and Innovation) grant no. PICT 2015-2437 to J.A.C. (2016 -2020). T32  
467 Training in Tropical and Emerging Global Diseases Grant (T32AI060546) and funding from the  
468 NIH (R01AI163140 and R01GM144545) to R.D.E..

469 JAC is a researcher of CONICET (National Research Council of Science and Technology), ET has  
470 a fellowship from CONICET to conduct her Ph.D., CBD had a PDRA position associated to grant  
471 agreement 'A Global Network for Neglected Tropical Diseases' grant number MR/P027989/1.

472

473 **Author contributions:**

474 J.A.C. and E.T. conceived, designed and supervised the project, E.T. performed most of  
475 designed experiments, C.B.D.C. performed qPCR assay, N.M.C obtained the microscopy  
476 images. J.A.C., E.T. and R.D.E. discussed the results. J.A.C. and E.T. wrote the manuscript with  
477 contributions from all other authors.

478

479 **Abbreviations:**

480 ANOVA: Analysis of variance, ConA: concanavalin A; FBS: Fetal Bovine Serum; FP: flagellar  
481 pocket; Hb: Hemoglobin; HRG: Heme Responsive Gene; IHC: Intracellular heme content; LIT:  
482 Liver Infusion Tryptose; PBS: Phosphate buffered saline; qRT-PCR: quantitative real-time PCR;  
483 rTcHRG: recombinant TcHRG; SPC: Citostome-cytopharinx complex; TcHRG, Trypanosoma  
484 cruzi Heme Response Gene; WT: Wild Type

485

486 **Conflict of interest:** The authors declare that they have no conflict of interest with the content  
487 of this article.

488

489 **FIGURE LEGENDS:**

490 **Figure 1: Endogenous *TcHRG* expression responds to Hb-derived heme in epimastigotes.** WT  
491 epimastigotes (Dm28c) were routinely cultured in LIT-10% FBS + 5  $\mu$ M hemin, then challenged  
492 to heme starvation for 48 h. After heme starvation, epimastigotes were collected, washed  
493 with PBS and transferred to culture media were supplemented with 5, 20, or 50  $\mu$ M hemin,  
494 1.25, 5, and 12.5  $\mu$ M Hb, or without heme (0  $\mu$ M).

495 (A) Growth curve of WT epimastigotes supplemented with Hb, with hemin or without the  
496 addition of heme source for 14 days. The number of cells was followed daily for 7 days. A  
497 dilution to the initial concentration in fresh medium as performed at day 7, and the growth  
498 curves were followed for another 7 days. Data are presented as mean  $\pm$  SD of three  
499 independent assays. Microcentrifuge tubes cartoons in different colors indicate sampling for  
500 Western blot (WB) analysis (black), quantitative PCR (qPCR) analysis (dark gray) and  
501 intracellular heme content (IHC) measurements (light gray) on the corresponding days.

502 (B) Detection of endogenous *TcHRG* by Western blot. Samples were taken on days 1, 3, 7, and  
503 14 over the course of the growth curves. Polyclonal anti-*TcHRG* antibodies were used to  
504 recognize endogenous protein in total extracts of epimastigotes. Detection of  $\alpha$ -tubulin was  
505 used as a loading control.

506 (C) Quantification of *TcHRG* mRNA levels in WT epimastigotes cultured in media with 5  $\mu$ M  
507 hemin, 1.25  $\mu$ M Hb or without heme source. Samples were taken at  $t_0$  (after heme starvation  
508 and prior incubating parasites in the different conditions) and  $t_{24}$  (24 h post treatment). mRNA  
509 was quantified by qRT-PCR. GAPDH was used for normalization. Data are presented as mean  
510  $\pm$  SD of three technical replica, expressed as the ratio of fold change of  $t_{24}$  to  $t_0$ . Statistical  
511 significance was determined by one-way ANOVA followed by Dunnett's multiple comparisons  
512 test (\*\*\*,  $p < 0.001$ ; \*\*,  $p < 0.01$ ).

513 (D) IHC determined by pyridine method of epimastigotes incubated in media with 5  $\mu$ M hemin  
514 or 1.25  $\mu$ M Hb. Samples were taken after 48 and 96 h of treatment. Data are presented as  
515 mean  $\pm$  SD of 3 independent assays. Statistical significance was determined by two-way  
516 ANOVA followed by Sidak's multiple comparisons test (\*\*\*\*,  $p < 0.0001$ ).

517 **Figure 2: Endocytic null epimastigotes are able to grow in Hb-supplemented medium and**  
518 **to reach WT intracellular heme values.** WT, *TcAct2* and *TcAct2.Ty* (Y strain) epimastigotes  
519 were routinely cultured in LIT-10% FBS + 5  $\mu$ M hemin, subjected to heme starvation for 48 h,  
520 as described previously, and finally transferred to media supplemented with 5  $\mu$ M hemin,

521 1.25  $\mu$ M Hb, or without heme source added (0  $\mu$ M) for one week. After 48 h, samples were  
522 taken to perform Western blot analysis and intracellular heme measurements.  
523 Microcentrifuge tubes cartoons indicate sampling for Western blot (WB) analysis (black), and  
524 intracellular heme content (IHC) measurements (light gray) on the corresponding days.

525 (A) Growth curve of WT, *TcAct2* and *TcAct2.Ty* epimastigotes cultured in media 5  $\mu$ M hemin,  
526 1.25  $\mu$ M Hb, or without heme added. The number of parasites was followed daily for one  
527 week. Data are presented as mean  $\pm$  SD of three independent assays.

528 (B) Western blot assay using anti-*TcHRG* antibodies to detect endogenous *TcHRG* protein in  
529 total extracts of WT, *TcAct2* and *TcAct2.Ty* epimastigotes incubated for 48 h in media  
530 supplemented with 5  $\mu$ M hemin, 1.25  $\mu$ M Hb or without heme source.  $\alpha$ -tubulin was used as  
531 a loading control.

532 (C) IHC determined by pyridine method of WT, *TcAct2* and *TcAct2.Ty* epimastigotes incubated  
533 for 48 h in media supplemented with 5  $\mu$ M hemin, 1.25  $\mu$ M Hb or without heme source. Data  
534 are presented as mean  $\pm$  SD of 3 independent assays. Statistical significance was determined  
535 by one-way ANOVA followed by Dunnett's multiple comparisons test. (\*\*\*\*,  $p < 0.0001$ ; \*\*\*,  
536  $p < 0.001$ ; \*\*,  $p < 0.01$ ).

537 **Figure 3: Overexpression of *TcHRG* leads to an increment on IHC in Hb-supplemented**  
538 **parasites.** Control epimastigotes (pLEW 13 p*TcIndex*) and *rTcHRG.His-GFP* expressing  
539 epimastigotes (pLEW 13 p*TcIndex.GW.TcHRG.His-GFP*) (Dm28c strain) were cultured in LIT-  
540 10% FBS + 5  $\mu$ M hemin, then challenged to heme starvation for 48 h and finally transferred  
541 to media supplemented with 5  $\mu$ M hemin or 1.25  $\mu$ M Hb for 48 h.

542 (A) IHC determined by pyridine method. Data are presented as mean  $\pm$  SD of 3 independent  
543 assays. Statistical significance was determined by two-way ANOVA followed by Sidak's  
544 multiple comparisons test. (\*\*\*\*,  $p < 0.0001$ ; \*\*\*,  $p < 0.001$ ).

545 (B) Western blot assay using anti-GFP antibodies to detect recombinant *TcHRG.His-GFP*  
546 protein in total extracts of *rTcHRG.His-GFP* overexpressing epimastigotes incubated for 48 h  
547 in the conditions mentioned above. Detection of  $\alpha$ -tubulin was used as a loading control.

548 **Figure 4: Localization of endogenous *TcHRG*.** Superresolution structured illumination (SR-  
549 SIM) microscopy of:

550 (A) Epimastigotes that express *rTcHRG.His-GFP* (Dm28c strain) cultured in LIT-10% FBS + 5  $\mu$ M  
551 hemin. Polyclonal anti-*TcHRG* antibodies (red) were used to validate specific union to

552 rTcHRG.His-GFP protein (green). The colocalization analysis (red:green) was performed  
553 (Pearson's coefficient: 0.821 and Manders' coefficients: 0.988 and 0.969).

554 (B) WT epimastigotes (Y strain) cultured in media supplemented with 5  $\mu$ M hemin (upper  
555 panel) or 1.25  $\mu$ M Hb (lower panel). anti-TcHRG antibodies were used as to recognize  
556 endogenous TcHRG protein (green). Labeling with concanavalin A-rhodamine (ConA, red) was  
557 used to identify the parasite's surface. No difference was observed between Y and Dm28c  
558 strain.

559 (C) WT epimastigotes (Y strain) cultured in medium supplemented with 5  $\mu$ M hemin.  $\alpha$ -TcHRG  
560 antibodies were used as to recognize endogenous TcHRG protein (green) and MitoTracker™  
561 Red CMXRos were used to label the mitochondria (red). The colocalization analysis  
562 (red:green) was performed. Pearson's coefficient: 0.545 and Manders' coefficients 0.801 and  
563 0.988 (Upper panel). Pearson's coefficient: 0.647 and Manders' coefficients 0.744 and 0.996  
564 (Lower panel).

565 (D) Scheme of TcHRG localization in WT epimastigotes. Nucleus and kinetoplast are  
566 schematized in blue, the flagellum and the cytostome entrance are depicted in red. TcHRG is  
567 schematized as green dots throughout the parasite's body and concentrated in the FP area.  
568 Nuclei and kinetoplasts in all fluorescent images were stained with DAPI (4,6-diamidino-2-  
569 phenylindole, blue). Scale bars: 5  $\mu$ m.

570 **Figure 5: Scheme of the proposed model of heme uptake in epimastigotes of *Trypanosoma***  
571 ***cruzi*.**

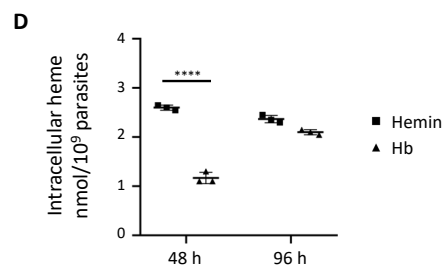
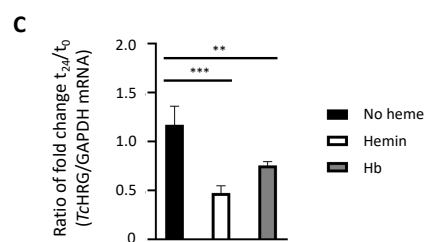
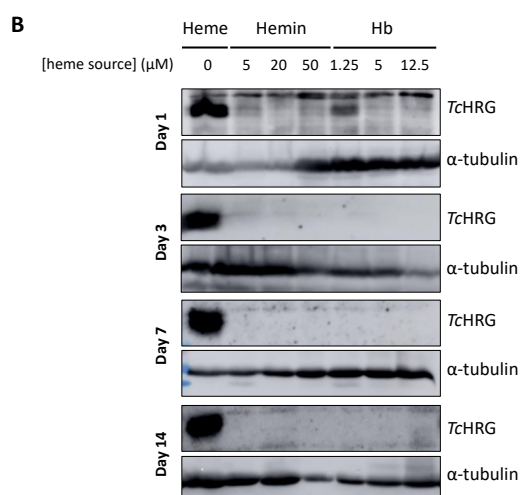
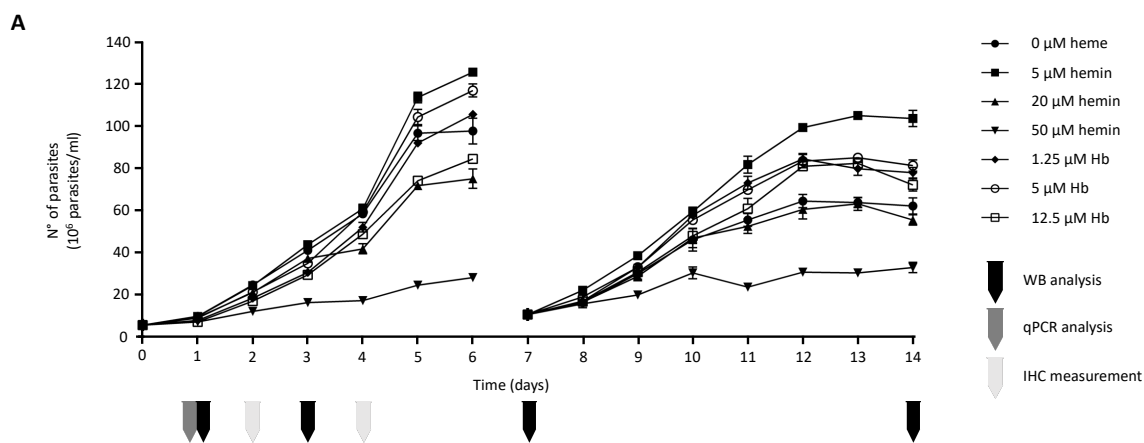
572 When the epimastigote senses that the IHC is below the optimal range, TcHRG expression  
573 increases, promoting the incorporation of heme derived from externally degraded Hb in the  
574 FP region. Heme should be then distributed and incorporated into hemoproteins, and  
575 mitochondrial TcHRG could also be involved in this process promoting heme transport to the  
576 mitochondria. Hb might also be endocytosed through the SPC and internally processed to  
577 obtain free heme, that may be exported to the cytosol or stored in reservosomes. Once the  
578 parasite obtains enough heme to satisfy its nutritional requirements, likely *via* intracellular  
579 TcHRG, its expression is downregulated to maintain heme homeostasis.

580

581 FIGURE 1:

582

583



584

585

586

587

588

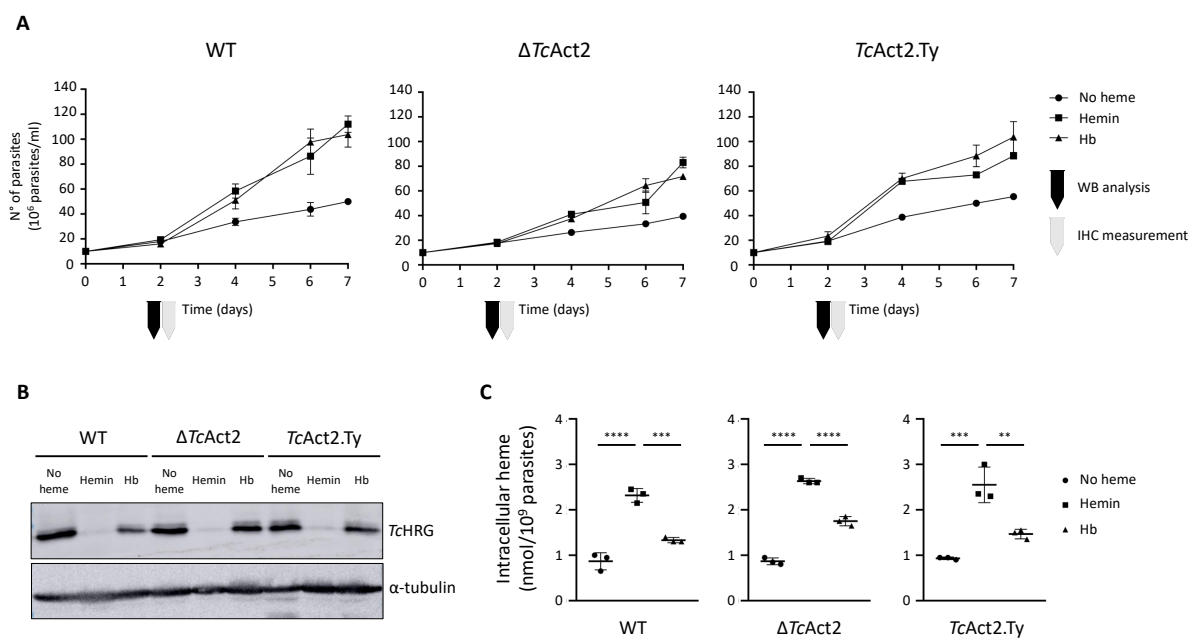
589

590

591 FIGURE 2

592

593



594

595

596

597

598

599

600

601

602

603

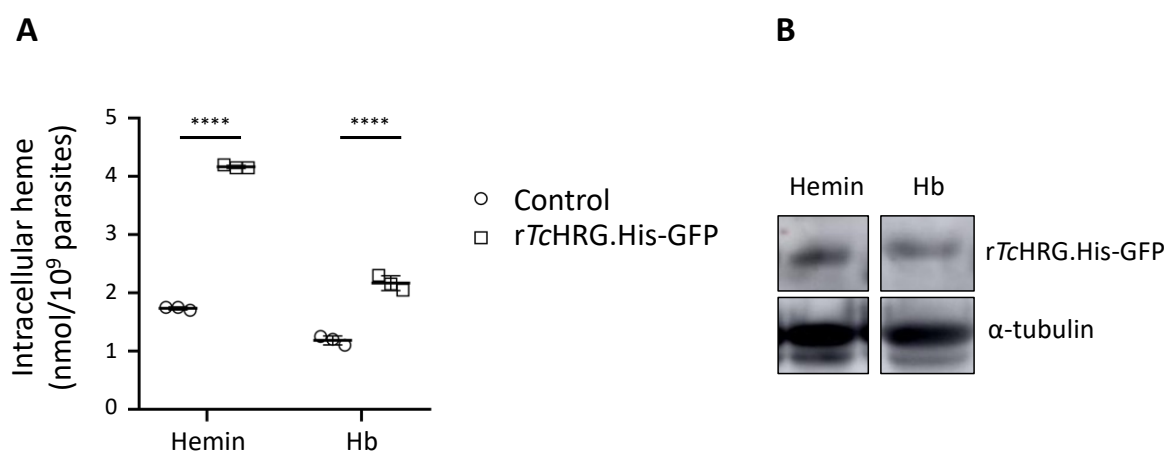
604

605

606

607 FIGURE 3

608



609

610

611

612

613

614

615

616

617

618

619

620

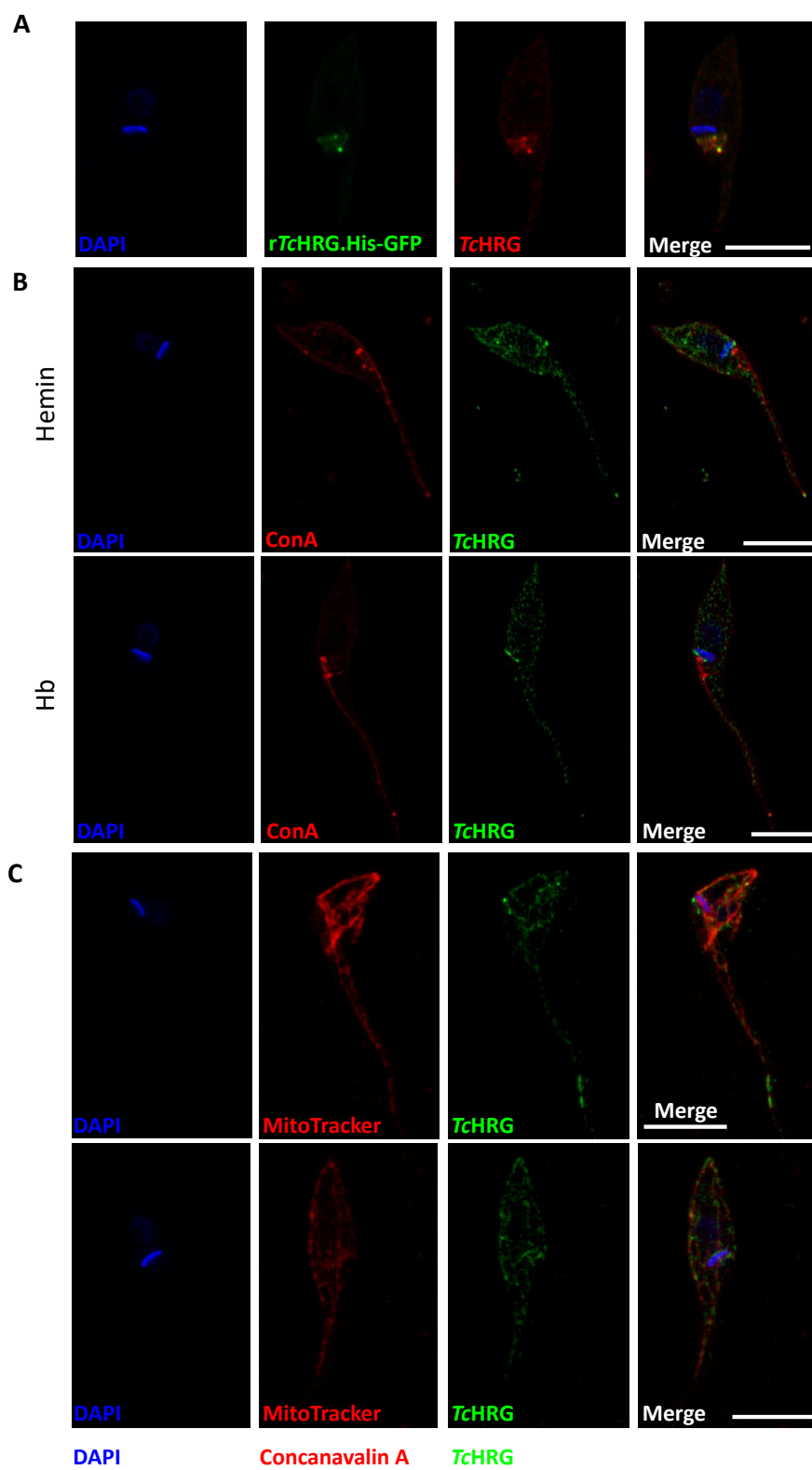
621

622

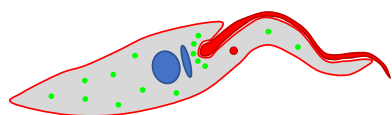
623

624

625 FIGURE 4



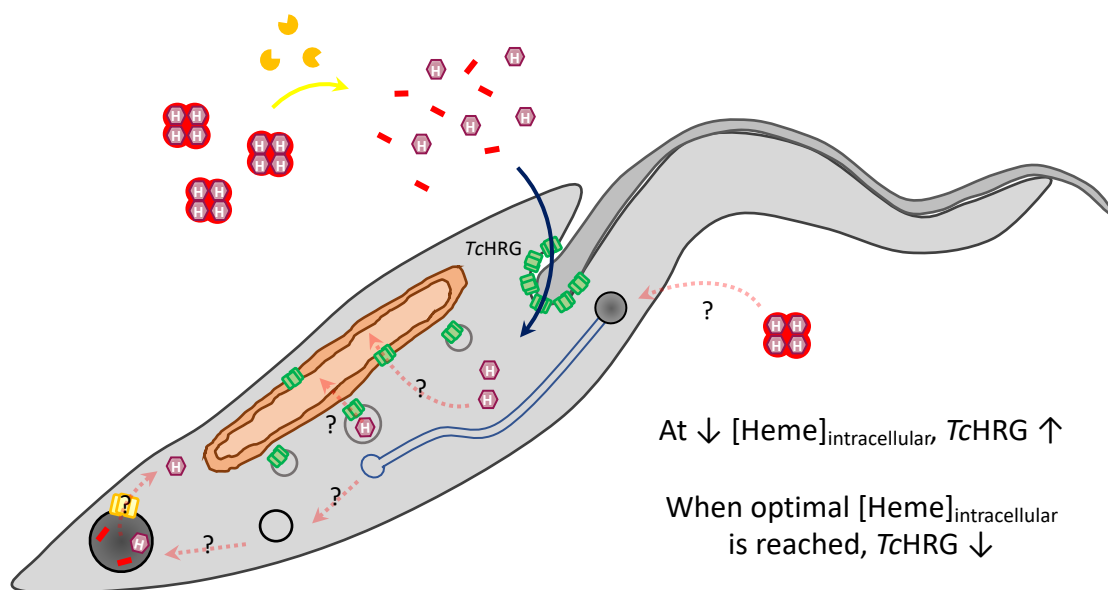
**D**



626

627 FIGURE 5

628



629

630

631

632

633